Nov 7th, 12:00 AM - Nov 8th, 12:00 AM

Web Crippling of Cold-Formed High Strength Steel Square and Rectangular Hollow Sections under Two-Flange Loading Conditions

Hai-Ting Li

Benjamin Young

Follow this and additional works at: https://scholarsmine.mst.edu/isccss

Part of the Structural Engineering Commons

Recommended Citation

Li, Hai-Ting and Young, Benjamin, "Web Crippling of Cold-Formed High Strength Steel Square and Rectangular Hollow Sections under Two-Flange Loading Conditions" (2018). *International Specialty Conference on Cold-Formed Steel Structures*. 5.
https://scholarsmine.mst.edu/isccss/24iccfss/session2/5

Web Crippling of Cold-Formed High Strength Steel Square and Rectangular Hollow Sections under Two-Flange Loading Conditions

Hai-Ting Li[1] and Ben Young[2]

Abstract

The web crippling behavior of cold-formed high strength steel (HSS) square and rectangular hollow sections under End-Two-Flange and Interior-Two-Flange loading conditions is studied. The cold-formed HSS tubular sections had nominal 0.2% proof stresses of 700 and 900 MPa. Finite element (FE) models were developed and validated against test results, showing the capability of replicating the experimental web crippling strengths, failure modes and load-deformation histories. Upon validation of the FE models, an extensive parametric study comprised 112 FE analyses was performed. The web crippling strengths obtained from the experimental and numerical investigations were compared with the nominal strengths calculated from the North American Specification, Australian/New Zealand Standard and European Code for cold-formed steel structures. The comparison results show that the nominal strengths predicted by the existing codified web crippling design provisions are either unconservative or overly conservative. Hence, new design rules are proposed for cold-formed HSS square and rectangular hollow sections by means of Direct Strength Method (DSM). It is shown that the modified DSM is able to provide reasonably good predictions.

Introduction

Cold-formed steel tubular sections, which are often difficult and uneconomical to be stiffened by transverse stiffeners, are vulnerable to web crippling failure when subjected to concentrated transverse forces. Many studies have been conducted to investigate the web crippling behavior of cold-formed steel open sections,

[1] Postdoctoral Fellow, Department of Civil Engineering, The University of Hong Kong, Pokfulam Road, Hong Kong, China.
[2] Professor, Department of Civil Engineering, The University of Hong Kong, Pokfulam Road, Hong Kong, China.

including recently introduced Direct Strength Method (DSM) based web crippling design rules by Gunalan & Mahendran (2015), Natário et al. (2016, 2017) and Heurkens et al. (2018). To date, however, investigation on cold-formed steel tubular sections undergoing web crippling is rather limited.

High strength steels have attracted attention in structural applications due to their excellent strength-to-weight ratios that could lead to lighter and elegant structures. The objective of this paper is to provide reliable design rules for cold-formed high strength steel (HSS) square and rectangular hollow sections subjected to web crippling under the two-flange loading conditions. Finite element (FE) models were developed and validated against the web crippling tests reported previously by the authors (Li & Young, 2017a). The End-Two-Flange (ETF) and Interior-Two-Flange (ITF) loading conditions, as specified in the North American Specification (NAS, 2016a) and Australian/New Zealand Standard (AS/NZS, 2005), were investigated. Upon validation of the FE models, an extensive parametric study was performed. The applicability of the codified web crippling provisions in the NAS (2016a), AS/NZS (2005) and European Code (EC3, 2006) to cold-formed HSS tubular sections was assessed. Web crippling design rules based on DSM are proposed for cold-formed HSS square and rectangular hollow sections under the codified two-flange loading conditions.

Experimental Investigation

Summary of Web Crippling Test Program

A total of 36 web crippling tests was conducted by the authors (Li & Young, 2017a) on cold-formed HSS tubular sections under the ETF and ITF loading conditions. The tests were carried out on square and rectangular hollow sections (SHS and RHS) with measured 0.2% proof stresses ranged from 679 to 1025 MPa (obtained from longitudinal tensile flat coupon tests). The measured section web slenderness ratios h/t ranged from 8.3 to 35.6, in which h is the depth of the web flat portion and t is the web thickness. The specimen lengths L were determined as per the NAS (2016a) and AS/NZS (2005). The loading or reaction forces were applied through steel bearing plates and the bearing plates were acted across full-flange widths excluding the corners of the sections. All flanges of the cold-formed SHS and RHS specimens were not fastened to the bearing plates. The web crippling test program is detailed in Li & Young (2017a).

Corner Coupon Tests

The material properties of the cold-formed HSS tubular specimens were obtained by coupon tests. Longitudinal tensile and transverse compressive flat coupon tests

were conducted, as reported by Li & Young (2017a). It should be noted that, due to cold-working, the corner regions of the cold-formed SHS and RHS were strengthened, and therefore, exhibited enhanced yield stresses and ultimate strengths compared to their flat counterparts. Hence, in order to obtain material properties of the highly cold-worked corners, longitudinal tensile corner coupon tests were conducted and are reported in the present study. The corner coupons were extracted from the SHS and RHS (opposite to the weld) in the longitudinal direction and an MTS material testing machine was used to conduct the tensile corner coupon tests. For each coupon test, the instrumentation comprised of two strain gauges and a calibrated 25 mm gauge length MTS extensometer. The tensile corner coupon specimens were loaded through two pins and the test procedures were in accordance with those described by Li & Young (2017a) for tensile flat coupon tests. Table 1 summarizes the material properties determined from the corner coupon tests, namely, Young's moduli (E_c), 0.2% proof stresses ($\sigma_{0.2,c}$), tensile strengths ($\sigma_{u,c}$) and fracture strains ($\varepsilon_{f,c}$) based on a 25 mm gauge length. The corner material properties were also incorporated in numerical modeling.

Table 1: Material properties obtained from corner coupon tests

Section ($H \times B \times t$)	E_c (GPa)	$\sigma_{0.2,c}$ (MPa)	$\sigma_{u,c}$ (MPa)	$\varepsilon_{f,c}$ (%)
H80×80×4	214.2	877	945	12.2
H120×120×4	213.0	875	952	11.6
H160×160×4	216.2	899	992	11.7
H50×100×4	207.2	860	932	11.8
H50×100×4-R[†]	203.9	868	955	11.9
V80×80×4	208.5	1151	1293	10.5
V100×100×4	219.6	1073	1175	11.1
V120×120×4	209.2	1079	1195	11.5

Note: [†]Repeated coupon test.

Numerical Modelling

The finite element (FE) program ABAQUS (2012) was used to develop FE models for simulating the web crippling tests that reported previously by the authors (Li & Young, 2017a). The FE models were built on the measured geometries of the test specimens. The four-node doubly curved shell element S4R was selected herein to simulate the cold-formed HSS tubular specimens. The steel bearing plates were modeled using discrete rigid 3D solid elements. The mesh sizes applied in the flat portions of the SHS and RHS ranged from 4×4 mm to 12×12 mm depending on the size of the sections and finer meshes at the round corners were employed. The elastic parts of the material properties were

represented by the measured Young's moduli with a Poisson's ratio of 0.3. For the inelastic parts, the material nonlinearities of the cold-formed HSS tubular sections were incorporated into the FE models by specifying true stress and true plastic strain data, which were based on the measured engineering stress-strain curves obtained from the coupon tests. In the FE models, the compressive flat material properties in the transverse direction were used for the webs of the SHS and RHS, whereas the tensile flat material properties were used for the flanges. The tensile corner material properties with the extension of $2t$ beyond the curved portions to the adjacent flat regions were applied in the FE models.

The boundary conditions were modeled in accordance with the web crippling tests. The transverse bearing forces (and reaction forces) were transferred to the tubular specimens through bearing plates. Contact pairs were used in the FE models to define the surface interactions between the tubular specimens and the bearing plates. The master and slave surfaces were defined in the rigid bearing plates and the deformable cold-formed HSS tubular specimens, respectively. It is noteworthy that the corner regions of the HSS tubular sections underwent large plastic deformations and contacted the bearing plates gradually during the tests. Hence, in the FE models, the corner elements were also included in the slave surfaces along with the flange elements. The "hard" contact was employed for the contact property in the normal direction. For the contact property in the tangential direction, the friction penalty contact with a friction coefficient of 0.4 was applied. The loads were applied to the HSS tubular specimens by specifying axial displacements to the reference points of the bearing plates, which was identical to the web crippling tests.

Validation of Finite Element Models

Web crippling strengths per web (P_{FEA}) derived from the FE analyses were compared with the corresponding experimental strengths per web (P_{Exp}) reported by Li & Young (2017a). The mean values of the $P_{\text{Exp}} / P_{\text{FEA}}$ were 0.99 and 0.98 with the corresponding coefficients of variation (COVs) of 0.067 and 0.044 for the ETF and ITF specimens, as shown in Tables 2 and 3, respectively. Typical numerical failure modes were compared with their experimental counterparts, as displayed in Figure 1. Typical load-deformation curves that derived numerically were also compared with their experimental counterparts, as shown in Figure 2. It can be concluded that the FE models, which make use of both flat and corner material properties, are capable of replicating the behavior of cold-formed HSS tubular sections undergoing web crippling.

Table 2: Comparison of test and FE strengths for ETF loading condition

Specimen	Test[^] P_{Exp} (kN)	FEA P_{FEA} (kN)	Comparison P_{Exp}/P_{FEA}
ETF-H80×80×4N90	75.7	81.6	0.93
ETF-H80×80×4N50	55.2	53.1	1.04
ETF-H120×120×4N120	79.6	81.9	0.97
ETF-H120×120×4N60	53.9	54.6	0.99
ETF-H160×160×4N150	72.6	77.3	0.94
ETF-H160×160×4N90	57.2	59.8	0.96
ETF-H50×100×4N90	100.0	94.0	1.06
ETF-H50×100×4N50-1	66.7	59.7	1.12
ETF-H50×100×4N50-2	66.6	59.7	1.12
ETF-H100×50×4N50	51.0	51.6	0.99
ETF-H100×50×4N30-1	38.3	37.8	1.01
ETF-H100×50×4N30-2	36.6	37.7	0.97
ETF-V80×80×4N90	87.3	91.0	0.96
ETF-V80×80×4N50	60.8	59.3	1.03
ETF-V100×100×4N90	66.6	76.2	0.87
ETF-V100×100×4N50	50.1	51.7	0.97
ETF-V120×120×4N120	77.5	86.1	0.90
ETF-V120×120×4N60	55.9	58.5	0.96
		Mean	0.99
		COV	0.067

Note: [^] Conducted by Li & Young (2017a).

Table 3: Comparison of test and FE strengths for ITF loading condition

Specimen	Test[^] P_{Exp} (kN)	FEA P_{FEA} (kN)	Comparison P_{Exp}/P_{FEA}
ITF-H80×80×4N90	137.7	141.5	0.97
ITF-H80×80×4N50	120.0	114.8	1.04
ITF-H120×120×4N120	152.9	157.6	0.97
ITF-H120×120×4N60	139.4	131.4	1.06
ITF-H160×160×4N150	164.0	172.1	0.95
ITF-H160×160×4N90	148.9	153.9	0.97
ITF-H50×100×4N90-1	144.2	148.2	0.97
ITF-H50×100×4N90-2	143.3	148.2	0.97
ITF-H50×100×4N50	118.1	112.4	1.05
ITF-H100×50×4N50	125.1	117.0	1.07
ITF-H100×50×4N30-1	98.9	104.3	0.95
ITF-H100×50×4N30-2	97.6	104.3	0.94
ITF-V80×80×4N90	164.3	168.9	0.97
ITF-V80×80×4N50	140.3	144.2	0.97
ITF-V100×100×4N90	150.7	155.2	0.97
ITF-V100×100×4N50	131.1	142.0	0.92
ITF-V120×120×4N120	175.9	182.5	0.96
ITF-V120×120×4N60	150.7	154.4	0.98
		Mean	0.98
		COV	0.044

Note: [^] Conducted by Li & Young (2017a).
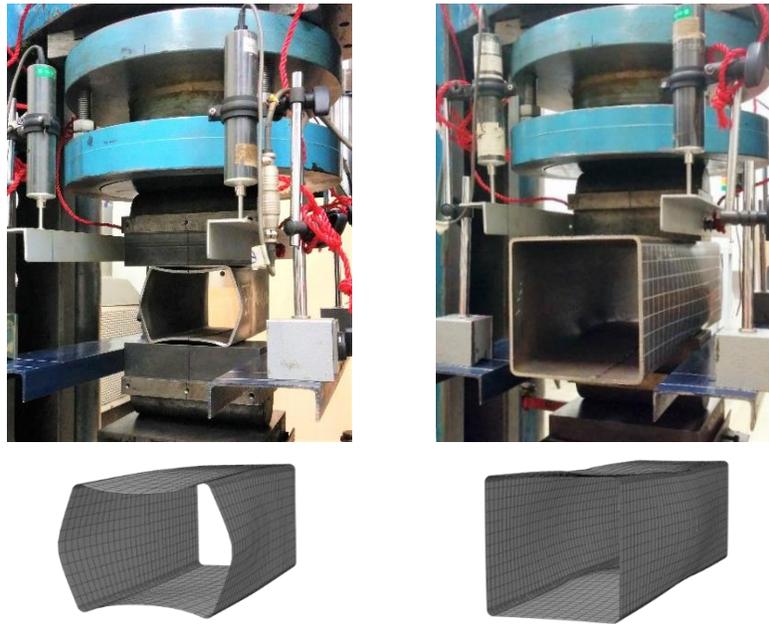
(a) ETF-H120×120×4N120   (b) ITF-H160×160×4N90
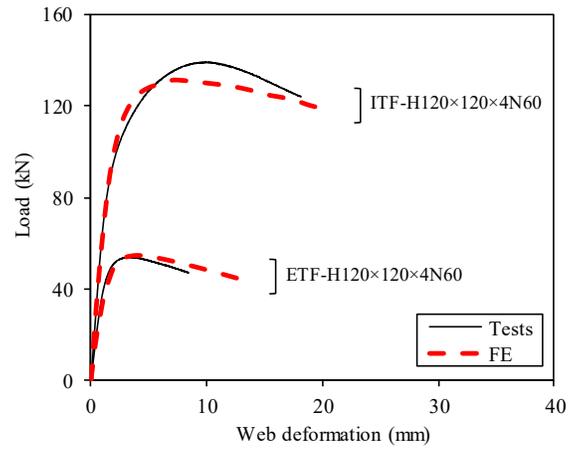
Figure 1: Typical experimental and numerical failure modes

Figure 2: Load-deformation curves for specimens ETF-H120×120×4N60 and
ITF-H120×120×4N60

Parametric Study

Upon validation, FE analyses were carried out using the validated FE models to generate numerical data covering a wide range of web slenderness ratios h/t, bearing length to web flat portion ratios N/h and bearing length to thickness ratios N/t. The parametric study performed in this study covered 16 SHS and 12 RHS, and these tubular sections were selected from the range of practical cross-section sizes for structural applications. The cross-sectional dimensions ($H \times B \times t$) of the HSS tubular sections varied between 150×150×4 and 400×200×8 with the h/t ratios ranged from 10 to 106, where H is the overall web height, B is the overall flange width, t is the thickness and h is the web flat portion depth. Two different bearing lengths (N) were designed for each cross-section and the N were either full or half of the overall flange width B. The N/h ratios varied between 0.3 and 1.5 and the N/t ratios ranged from 7.5 to 110.0. The specimen lengths in the parametric study were determined in accordance with the NAS (2016a) and AS/NZS (2005).

Similar to the test program (Li & Young, 2017a), the cold-formed HSS square and rectangular hollow sections investigated in the parametric study covered two steel grades: 700 and 900 MPa, being referred as "H" and "V" series, respectively. The measured material properties of the sections H160×160×4 and V100×100×4 were used for the "H" and "V" series, respectively. The compressive flat material properties were used for the webs, while the tensile flat material properties were used for the flanges of the HSS tubular sections. The tensile corner material properties were applied to the curved corners of the sections with the extension of $2t$ to the adjacent flat regions. A total of 112 results were generated in the parametric study.

Existing Design Provisions and Comparison with Web Crippling Strengths

The applicability of the codified web crippling provisions, as given in the NAS (2016a), AS/NZS (2005) and EC3 (2006), to cold-formed HSS square and rectangular hollow sections was evaluated by comparing the test and FE strengths per web (P_u) with the nominal strengths per web calculated from these provisions. The tensile and compressive material properties of flat coupons, as detailed in Li & Young (2017a), were used to calculate the nominal strengths per web P_{pred}^{T} and P_{pred}^{C} for the NAS (2016a), AS/NZS (2005) and EC3 (2006), respectively. The comparison of the P_u with the P_{pred}^{T} and the P_{pred}^{C} for the ETF and ITF specimens are shown in Tables 4 and 5.

North American Specification

Purely theoretical analysis for cold-formed steel members undergoing web crippling has been found quite complicated (NAS, 2016b). The provisions in the NAS (2016a) for members subjected to web crippling are empirical, which have been developed based on experimental investigations carried out since the 1940s. A unified equation has been used by the NAS (2016a) for web crippling check of cold-formed steel sections. The unified equation is capable of accommodating various cross-section geometries through different sets of coefficients.

Overall, the nominal strengths per web, P_{NAS}^{T} and P_{NAS}^{C}, that calculated using the 0.2% proof stresses from tensile and compressive flat coupon tests, respectively, were unconservative, as shown in Tables 4 and 5. The mean values of the test and FE-to-predicted strength ratios P_{u}/P_{NAS}^{T} were 0.62 and 0.68 with the corresponding COVs of 0.202 and 0.162 for the ETF and ITF specimens, respectively. The mean values of the P_{u}/P_{NAS}^{C} were 0.55 and 0.60 with the COVs of 0.206 and 0.168 for the ETF and ITF specimens, respectively.

Australian/New Zealand Standard

The AS/NZS (2005) has adopted its web crippling provisions from the NAS (the 2001 edition). Although the NAS has been revised three times in 2007, 2012 and 2016, the web crippling coefficients were updated only for built-up sections and multi-web deck sections. Therefore, the web crippling strengths of the cold-formed HSS tubular sections predicted by the NAS (2016a) and AS/NZS (2005) are identical.

European Code

The EC3 (2006) provides provisions to calculate the web crippling strength (known as the local transverse resistance of the web) for cold-formed steel sections. According to Figure 6.9 of the EC3 (2006), the ETF and ITF loading conditions that specified in the NAS (2016a) and AS/NZS (2005) belong to Category 1 in the EC3 (2006). The web crippling coefficient used in this study was 0.057 for the Category 1.

The nominal strengths per web predicted by the EC3 (2006) had great conservatism. The mean values of the P_{u}/P_{EC3}^{T} were 2.58 and 6.39 with the corresponding COVs of 0.247 and 0.159 for the ETF and ITF specimens, respectively. Similar results were also found for the P_{u}/P_{EC3}^{C}, as shown in Tables 4 and 5. It should be noted that, although the cold-formed HSS tubular sections

were loaded with various bearing lengths, the provisions in the EC3 (2006) for cross-sections with two or more unstiffened webs used a constant bearing length of 10 mm in calculating the web crippling strengths for the ETF and ITF (Category 1) specimens. In this study, it was found that the web crippling strengths could be increased by 66% and 31% through increasing the bearing lengths for the ETF and ITF loading conditions, respectively. Therefore, it is worth to compare the design predictions using the actual bearing lengths instead of 10 mm as specified in the EC3 (2006).

The P_u were compared with the $P_{EC3\#}^T$ and $P_{EC3\#}^C$ that calculated using the actual bearing lengths, as shown in Tables 4 and 5. The mean values of the $P_u/P_{EC3\#}^T$ were 1.52 and 3.74 with the corresponding COVs of 0.234 and 0.127 for the ETF and ITF specimens, respectively. The mean values of the $P_u/P_{EC3\#}^C$ were 1.40 and 3.45 with the corresponding COVs of 0.225 and 0.132 for the ETF and ITF specimens, respectively. Overall, the EC3 (2006) provided quite conservative predictions for the ETF and ITF loading conditions when the actual bearing lengths were used in the calculations. It should be noted that, for a given tubular section, web crippling strengths predicted by the EC3 (2006) for the ETF and ITF loading conditions, using either the actual values or 10 mm as the bearing length, will be identical. This is due to the reason that these two loading conditions that specified in the NAS (2016a) and AS/NZS (2005) belong to the same category according to the EC3 (2006).

Table 4: Comparison results for ETF loading condition

ETF	NAS		EC3				DSM	
No. of tests: 18 No. of FE: 56	$\dfrac{P_u}{P_{NAS}^T}$	$\dfrac{P_u}{P_{NAS}^C}$	$\dfrac{P_u}{P_{EC3}^T}$	$\dfrac{P_u}{P_{EC3}^C}$	$\dfrac{P_u}{P_{EC3\#}^T}$	$\dfrac{P_u}{P_{EC3\#}^C}$	$\dfrac{P_u}{P_{DSM}^T}$	$\dfrac{P_u}{P_{DSM}^C}$
Mean	0.62	0.55	2.58	2.38	1.52	1.40	1.08	1.00
COV	0.202	0.206	0.247	0.246	0.234	0.225	0.134	0.140

Table 5: Comparison results for ITF loading condition

ITF	NAS		EC3				DSM	
No. of tests: 18 No. of FE: 56	$\dfrac{P_u}{P_{NAS}^T}$	$\dfrac{P_u}{P_{NAS}^C}$	$\dfrac{P_u}{P_{EC3}^T}$	$\dfrac{P_u}{P_{EC3}^C}$	$\dfrac{P_u}{P_{EC3\#}^T}$	$\dfrac{P_u}{P_{EC3\#}^C}$	$\dfrac{P_u}{P_{DSM}^T}$	$\dfrac{P_u}{P_{DSM}^C}$
Mean	0.68	0.60	6.39	5.90	3.74	3.45	1.08	1.00
COV	0.162	0.168	0.159	0.168	0.127	0.132	0.121	0.135

Modified Direct Strength Method and Comparison with Web Crippling Strengths

The nominal web crippling strengths predicted by the NAS (2016a), AS/NZS (2005) and EC3 (2006) were either generally unconservative or overly conservative for the cold-formed HSS square and rectangular hollow sections. Therefore, improved design rules are proposed for the cold-formed HSS tubular sections undergoing web crippling in this study. Direct Strength Method (DSM) was introduced into the North American Specification since 2004. However, the current international standards, including the NAS (2016a), do not provide provisions for members undergoing web crippling based on DSM. Recently, attempts have been made by other researchers (e.g., Gunalan & Mahendran, 2015; Natário et al., 2016; Heurkens et al., 2018) applying DSM to cold-formed steel sections undergoing web crippling. It is noteworthy that these attempts were focused on cold-formed steel open sections only. The authors have previously proposed DSM for cold-formed ferritic stainless steel tubular sections undergoing web crippling for end loading (EL) and interior load (IL) conditions (Li & Young, 2017b). In this study, the DSM is modified for cold-formed HSS square and rectangular hollow sections subjected to the two-flange loading conditions (ETF and ITF). To develop DSM for members undergoing web crippling, bearing buckling strength P_{cr} and bearing yield strength P_y are needed for determining the web crippling strength P_{DSM}. The determination of the P_{cr} and P_y in Clause 5.13 of the AS4100 (1998) are adopted in this study. However, it should be noted that the P_{cr} and P_y in the AS4100 (1998) were developed for EL and IL conditions only instead of the codified two-flange loading conditions in the NAS (2016a) and AS/NZS (2005).

To obtain the P_{cr}, the webs were treated in the same way as columns subjected to compression. The "column" length was equal to the web flat portion h. The cross-sectional area of the "column" was taken as a mechanism length N_m multiplied by the web thickness t. The employed section constant value α_b was 0.5 and the form factor k_f of 1.0 was used. The geometrical slenderness ratios were taken as $3.8h/t$ and $3.5h/t$ for the ETF and ITF loading conditions, respectively. The bearing buckling strengths per web for cold-formed square and rectangular hollow sections can be computed by the following equation:

$$P_{cr} = \alpha_c t N_m \sigma_{0.2} \tag{1}$$

in which, α_c is the slenderness reduction factor which can be calculated from the Clause 6.3.3 of the AS4100 (1998); N_m is the mechanism length as expressed in Eq. (2).

$$N_{\mathrm{m}} = \begin{cases} N + 2.5R + 0.5h & \text{for ETF} \\ N + 5R + h & \text{for ITF} \end{cases} \tag{2}$$

in which, N is the bearing length; R is outer corner radius; h is the web flat portion.

The codified P_{y} of SHS and RHS webs as per the AS4100 (1998) were based on yield line mechanism analyses performed by Zhao & Hancock (1992, 1995). It should be noted that the web crippling loading conditions studied by Zhao & Hancock (1992, 1995) are not identical to the codified loading conditions in NAS (2016a) and AS/NZS (2005). In this study, the mechanism model proposed by Zhao & Hancock (1995) was used in the P_{y} calculations for the ETF and ITF loading conditions. This is due to the reason that the failure modes observed from the ETF and ITF specimens were similar to the mechanism model proposed by Zhao & Hancock (1995). The bearing yield strengths per web can be obtained as follows:

$$P_{\mathrm{y}} = \alpha_{\mathrm{p}} t N_{\mathrm{m}} \sigma_{0.2} \tag{3}$$

$$\alpha_{\mathrm{p}} = \sqrt{2 + k_{\mathrm{s}}^2} - k_{\mathrm{s}} \tag{4}$$

in which, $k_{\mathrm{s}} = 2R/t\text{-}1$.

The proposed web crippling strength per web, P_{DSM}, based on the DSM is shown in Eq. (5), which was previously proposed by Li & Young (2017b) for cold-formed ferritic stainless steel tubular sections. The modified coefficients a, b, n, λ_{k} and γ for cold-formed HSS tubular sections under ETF and ITF loading conditions are tabulated in Table 6. The validity limits are $690 \leq \sigma_{0.2} < 1200$ MPa, $10 \leq h/t \leq 110$, $r/t \leq 1.7$, $N/t \leq 110$, $N/h \leq 2.7$ and $\theta = 90°$.

$$P_{\mathrm{DSM}} = \begin{cases} \gamma \cdot P_{\mathrm{y}} & \lambda \leq \lambda_{\mathrm{k}} \\ a\left[1 - b\left(\dfrac{P_{\mathrm{cr}}}{P_{\mathrm{y}}}\right)^n\right]\left(\dfrac{P_{\mathrm{cr}}}{P_{\mathrm{y}}}\right)^n P_{\mathrm{y}} & \lambda > \lambda_{\mathrm{k}} \end{cases} \tag{5}$$

in which, $\lambda = (P_{\mathrm{y}}/P_{\mathrm{cr}})^{0.5}$ is the web crippling slenderness ratio.

Figures 3 and 4 show the comparisons of P_{u} with P_{DSM} for the ETF and ITF specimens, respectively. In Figures 3 and 4, the data points calculated using the tensile and compressive flat material properties were indicated by "(T)" and "(C)" in their figure legends, respectively. The mean values of the $P_{\mathrm{u}}/P_{\mathrm{DSM}}^{\mathrm{T}}$ were 1.08 and 1.08 with the COVs of 0.134 and 0.121 for the ETF and ITF specimens,

respectively, as shown in Tables 4 and 5. The mean values of the P_u/P_{DSM}^C were 1.00 and 1.00 with the COVs of 0.140 and 0.135 for the ETF and ITF specimens, respectively. It can be concluded that the modified DSM provided reasonably good predictions for cold-formed HSS tubular sections undergoing web crippling.
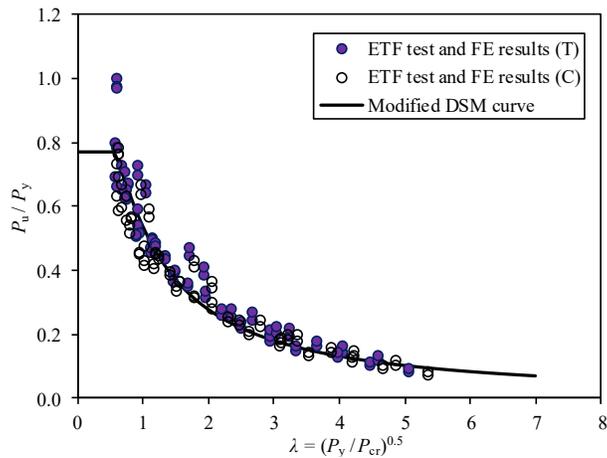

Figure 3: Comparison of test and FE results with modified DSM curve for ETF loading condition
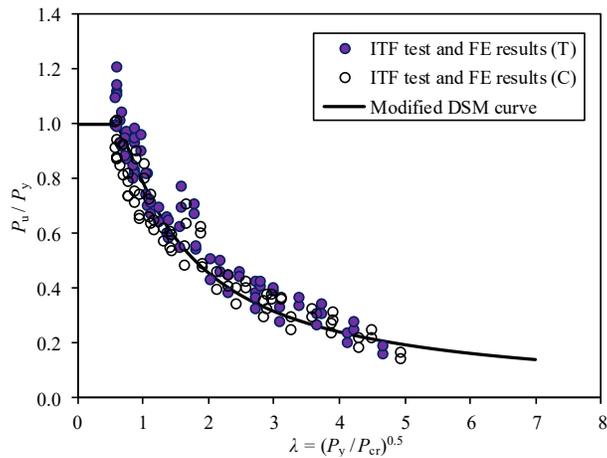

Figure 4: Comparison of test and FE results with modified DSM curve for ITF loading condition

Table 6: Proposed coefficients for design rules based on DSM

Load cases	a	b	n	λ_k	γ
ETF	0.69	0.22	0.58	0.560	0.77
ITF	1.08	0.27	0.52	0.566	1.00

Note: The above coefficients apply when $690 \leq \sigma_{0.2} < 1200$ MPa, $10 \leq h/t \leq 110$, $r/t \leq 1.7$, $N/t \leq 110$, $N/h \leq 2.7$ and $\theta = 90°$.

Conclusions

Cold-formed high strength steel (HSS) square and rectangular hollow sections undergoing web crippling have been investigated. The End-Two-Flange and Interior-Two-Flange loading conditions as specified in the North American Specification (NAS, 2016a) and Australian/New Zealand Standard (AS/NZS, 2005) for cold-formed steel structures were studied. Nonlinear finite element (FE) models were developed and validated against test results. Upon validation of the FE models, an extensive parametric study comprised 112 FE analyses was performed. The applicability of the codified provisions in the NAS (2016a), AS/NZS (2005) and European Code (EC3, 2006) to cold-formed HSS square and rectangular hollow sections was assessed. Overall, it is shown that the existing codified web crippling provisions were either unconservative or overly conservative for the cold-formed HSS tubular sections. A modified Direct Strength Method (DSM) has been proposed in this study to facilitate the design of cold-formed HSS tubular sections undergoing web crippling. It has been shown that the modified DSM, underpinned by 148 experimental and numerical data, were able to provide reasonably good predictions for cold-formed HSS tubular sections under the two-flange loading conditions.

Acknowledgment

Appendix. – References

ABAQUS. (2012). Abaqus/Standard user's manual volumes I-III and Abaqus CAE manual. Version 6.12. Hibbitt, Karlsson & Sorensen, Inc., Pawtucket, USA.

AS4100. (1998). Steel structures. AS 4100, Standards Australia, Sydney, Australia.

AS/NZS. (2005). Cold-formed steel structures. AS/NZS 4600, Standards Australia, Sydney, Australia.

EC3. (2006). Eurocode 3: Design of steel structures – Part 1-3: General rules – Supplementary rules for cold-formed members and sheeting. EN 1993-1-3, European Committee for Standardization, Brussels, Belgium.

Gunalan, S. and Mahendran, M. (2015). Web crippling tests of cold-formed steel channels under two flange load cases. Journal of Constructional Steel Research, 110: 1–15.

Heurkens, R.A.J., Hofmeyer, H., Mahendran, M. and Snijder, H.H. (2018). Direct strength method for web crippling – Lipped channels under EOF and IOF loading. Thin-Walled Structures. 123: 126–141.

Li, H.T. and Young, B. (2017a). Tests of cold-formed high strength steel tubular sections undergoing web crippling. Engineering Structures, 141: 571–583.

Li, H.T. and Young, B. (2017b). Cold-formed ferritic stainless steel tubular structural members subjected to concentrated bearing loads. Engineering Structures, 145: 392–405.

NAS. (2016a). North American Specification for the design of cold-formed steel structural members. AISI S100-16, American Iron and Steel Institute, Washington, D.C., USA.

NAS. (2016b). Commentary on North American Specification for the design of cold-formed steel structural members. AISI S100-16-C, American Iron and Steel Institute, Washington, D.C., USA.

Natário, P., Silvestre, N. and Camotim, D. (2016). Direct strength prediction of web crippling failure of beams under ETF loading. Thin-Walled Structures, 98: 360–374.

Natário, P., Silvestre, N. and Camotim, D. (2017). Web crippling of beams under ITF loading: A novel DSM-based design approach. Journal of Constructional Steel Research, 128: 812–824.

Zhao, X.L. and Hancock, G.J. (1992). Square and rectangular hollow sections subject to combined actions. Journal of Structural Engineering, 118(3): 648–668.

Zhao, X.L. and Hancock, G.J. (1995). Square and rectangular hollow sections under transverse end-bearing force. Journal of Structural Engineering, 121(9): 1323–1329.

Appendix. – Notation

B = Overall width of cross-section;
E = Young's modulus;
E_c = Young's modulus obtained from tensile corner coupon test;
H = Overall depth of cross-section;
L = Specimen length;

N	=	Bearing length;
N_{m}	=	Mechanism length;
P^{C}	=	Nominal web crippling strength per web calculated using compressive flat material properties;
P^{T}	=	Nominal web crippling strength per web calculated using tensile flat material properties;
P_{DSM}	=	Nominal web crippling strength per web obtained from the modified direct strength method;
$P_{\mathrm{DSM}}^{\mathrm{C}}$	=	Nominal web crippling strength per web obtained from the modified direct strength method using compressive flat material properties;
$P_{\mathrm{DSM}}^{\mathrm{T}}$	=	Nominal web crippling strength per web obtained from the proposed direct strength method using tensile flat material properties;
P_{EC3}	=	Nominal web crippling strength per web obtained from European Code;
$P_{\mathrm{EC3}}^{\mathrm{C}}$	=	Nominal web crippling strength per web obtained from European Code using compressive flat material properties;
$P_{\mathrm{EC3}}^{\mathrm{T}}$	=	Nominal web crippling strength per web obtained from European Code using tensile flat material properties;
P_{Exp}	=	Experimental web crippling strength per web;
P_{FEA}	=	Web crippling strength per web obtained from finite element analysis;
$P_{\mathrm{NAS}}^{\mathrm{C}}$	=	Nominal web crippling strength per web obtained from North American Specification using compressive flat material properties;
$P_{\mathrm{NAS}}^{\mathrm{T}}$	=	Nominal web crippling strength per web obtained from North American Specification using tensile flat material properties;
P_{cr}	=	Nominal bearing buckling strength per web;
P_{m}	=	Mean value of test and finite element strength to design prediction ratios;
P_{u}	=	Test and finite element strengths per web;
P_{y}	=	Nominal bearing yield strength per web;
R	=	Outer corner radius;
h	=	Depth of web flat portion;
t	=	Web thickness;
$\varepsilon_{\mathrm{f,c}}$	=	Fracture strain obtained from tensile corner coupon test based on 25 mm gauge length;
$\varepsilon_{\mathrm{u,c}}$	=	Ultimate strain obtained from tensile corner coupon test;
λ	=	Web crippling slenderness ratio;
$\sigma_{0.2}$	=	0.2% proof stress;
$\sigma_{0.2,\mathrm{c}}$	=	0.2% proof stress obtained from tensile corner coupon test; and
$\sigma_{\mathrm{u,c}}$	=	Tensile strength obtained from tensile corner coupon test.